Int. J. Electrochem. Sci., 6 **(2011)** 830 - 846

International Journal of
ELECTROCHEMICAL
SCIENCE
www.electrochemsci.org

In-Situ Study of Single and Double Loop Reactivation Methods During the Characterisation of the Degree of Sensitisation of a Duplex Stainless Steel (UNS 1.4462) Using a Minicell and a Confocal Microscope

R. Leiva-García[1], *M.J. Muñoz-Portero*[1], *J. García-Antón*[1,*]

[1] Ingeniería Electroquímica y Corrosión (IEC) Departamento de Ingeniería Química y Nuclear, E.T.S.I. Industriales, Universidad Politécnica de Valencia E-46071 Valencia, Spain
[*]E-mail: jgarciaa@iqn.upv.es

Received: 29 January 2011 / *Accepted:* 8 February 2011 / *Published:* 1 March 2011

The aim of this work is to study the evolution of the electrode surface during the single and double reactivation methods at microscopic scale. The tested material has been a duplex stainless steel (UNS 1.4462) in its as-received state and heated at 825 ºC for 1 hour in an inert atmosphere. Tests have been carried out in an electrochemical minicell that can be put in the stage of a confocal microscope. These devices allow the in-situ observation of the electrode surface at microscopic scale during the tests. Differences in the evolution of the electrode surface have been observed between the single and the double loop methods. Furthermore, the sensitised sample shows different evolution during the electrochemical tests than the as-received sample. These differences are due to the formation of new phases during the heat treatment. Therefore, the minicell permits obtaining additional information during the electrochemical characterisation of the degree of sensitisation in duplex stainless steels.

Keywords: Stainless steel, intergranular corrosion, sensitisation, confocal microscopy

1. INTRODUCTION

Stainless Steels have a good combination of mechanical properties and corrosion resistance. These properties can deteriorate if steels are sensitised to *intergranular corrosion*. Improper heat treatments at elevated temperatures or slow cooling from high temperatures can cause microstructural changes that lead to a decrease in corrosion resistance due to the formation of chromium depleted areas [1-11]. Among stainless steels, duplex stainless steels are considered a very attractive structural materials due to their good mechanical and corrosion resistance properties. Compared to austenitic

stainless steels, duplex stainless steels exhibit higher mechanical strength, comparable corrosion resistance and lower cost due to the reduced Ni content. In the case of duplex stainless steels, the higher Cr and Mo content, that improve the corrosion resistance, can promote the precipitation of secondary phases, such as sigma phase, when the steels are heated at elevated temperatures. These secondary phases, which are rich in alloying elements, lead to the depletion of adjacent areas in alloying elements.

There are a number of standard methods, such as oxalic acid test, Strauss test, Huey test, Streicher test, and Copper–Copper Sulfate-50 % sulphuric acid test, which can be used to assess susceptibility to intergranular corrosion according to ASTM A-262 [12]. None of these methods are quantitative and non-destructive methods. Moreover, performing the above mentioned tests is time consuming.

During the past decades, much research has been conducted to develop electrochemical potentiokinetic reactivation tests (EPR). Electrochemical potentiokinetic reactivation tests (single and double loop) have been widely employed to determine the degree of sensitisation of stainless steels [10, 13-17]. In these electrochemical tests, the aim is to reveal the surroundings of the precipitates, where the chromium concentration decreases below a critical value in order to obtain quantitative electrochemical parameters of the degree of sensitisation.

Resolution of electrochemical reactivations tests depends on several factors, such as acid and depassivator concentration, temperature, scan rate, reverse potential, and steel composition. This is the reason why the single loop method for AISI 304 and AISI 304L is the only standardised method. Some authors have tried to improve the resolution of these methods using statistical analysis [18]. Therefore, it could be interesting to observe the sample surface during the electrochemical reactivation tests in order to establish the evolution of the surface during the different steps of the tests relating surface images to electrochemical signals.

In a previous work [17], sample surface was observed during electrochemical potentiokinetic reactivation tests using the patented electro-optical devices P-200002525 and P-200002526 [19-22]. Images obtained during single and double loop electrochemical methods showed that both tests follow different passivation processes.

In the single loop test, surface modification happened later than the passivation process, and only, if the specimen was sensitised. In the double loop test, surface modification was produced before passivation. In order to improve the resolution of the patented electro-optical devices (the maximum magnification is 70X), an electrochemical minicell that can be accommodated in a confocal laser scanning microscope was developed in another work [23]. This minicell permits observing the electrode surface at higher magnifications than the previous devices.

Therefore, the goal of this paper is to characterise in-situ single and double loop electrochemical potentiokinetic reactivation tests at microscopic scale in a duplex stainless steel ,Alloy 900 (UNS 1.4462), in the as-received and sensitised state (heated at 825 ºC for 1 hour in an inert argon atmosphere) using a minicell accommodated in a confocal microscope. Additional analysis was performed by scanning electron microscopy (SEM), and X-ray diffraction analysis (EDX).

2. EXPERIMENTAL PROCEDURE

2.1. Working electrodes

The material used in this work was a duplex stainless steel, Alloy 900 (UNS 1.4462). The chemical composition in weight of Alloy 900 is: 22.34 % Cr, 4.85 % Ni, 1.59 % Mn, 0.35 % Si, 2.69 % Mo, 0.13 % Cu, 67.80 % Fe, 0.02 % P, 0.03 % C, 0.20 % N, and 0.01 % Ti. The Alloy 900 electrodes were machined as shown in Figure 1. These electrodes present a hole in the base, where the electrical connection was made, and a cylindrically reduced bar 1.6 mm in diameter.

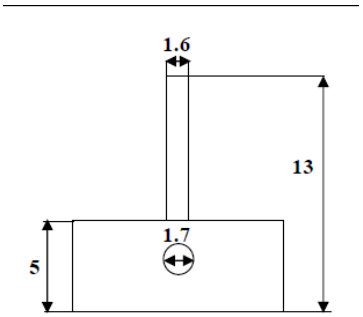

Figure 1. Machined working electrode of Alloy 900 (measurements in millimetres).

Three samples of Alloy 900 were introduced in a silica tube in a furnace (CARBOLITE TVS 12/600) under an argon atmosphere. The furnace is controlled by the software "*iTools*". Then, the samples were heated to develop sensitisation. Heat treatments have been carried out at 825 ºC for 1 hour; this heat treatment was selected because in previous works it caused sensitisation of Alloy 900 [8, 17]. Finally, the samples were water quenched. After the heat treatment, the electrodes were covered with an epoxy-resin; in this way only a circular area of 1.6 mm in diameter was exposed to the test solution (the area of the electrodes was determined for every test by image analysis). The electrical connection to the potentiostat was done by means of a conductor wire. Prior to the electrochemical tests, the specimens were wet abraded from 220 SiC (Silicon Carbide) grit to a 4000 SiC grit finish, and finally rinsed with distilled water.

2.2. Minicell description

Figure 2 shows a scheme of the minicell developed in a previous work [23] that permits using the confocal laser scanning microscopy in order to observe at microscopic scale the electrode surface during the tests. The cell is made of glass and consists of two parts. The first part is a base to support the specimens. This base has four small supports to maintain the working electrode in a horizontal position (Figure 2 c)), and a frosted lateral surface to close the cell with the upper part. The upper part has the inlets and outlets of the cell. There are two inlets for the electrodes, the first of them is for the

reference electrode, which is a silver-silver chloride with 3M KCl reference mini-electrode, and the second inlet serves to take out the electrical connection of the working electrode. The counter electrode consists of two platinum filaments that pass through the glass and are connected outside the cell to the potentiostat.

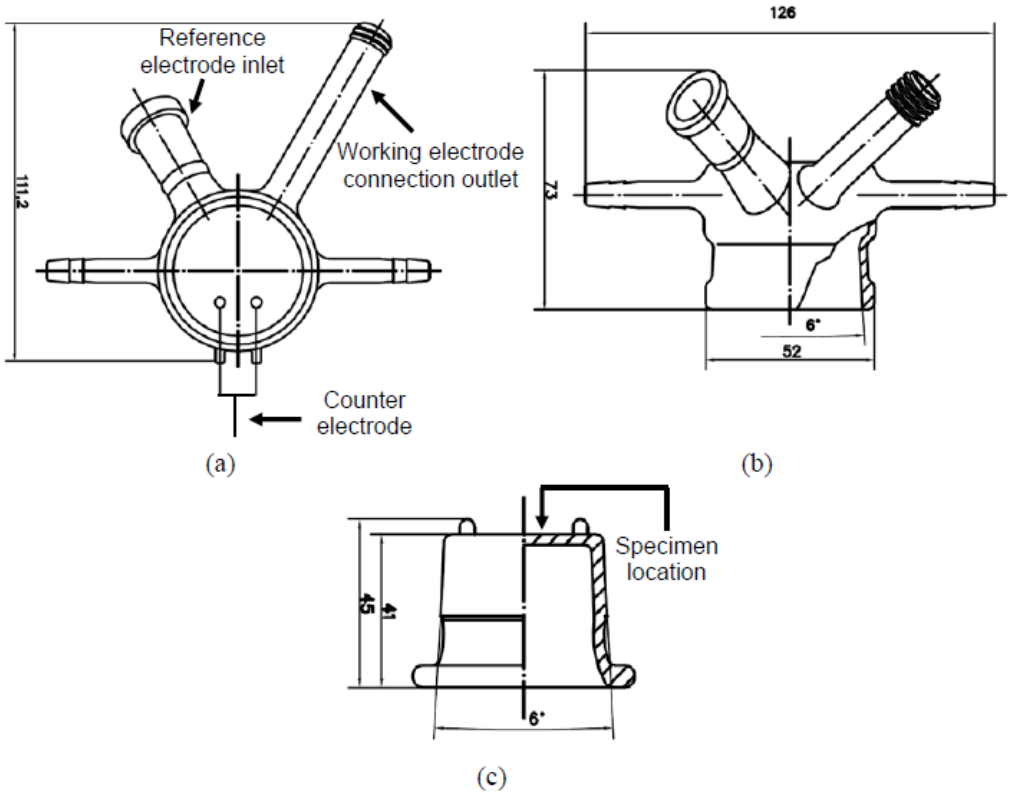

Figure 2. Scheme of the parts of the minicell: (a) Main view of the top of the cell, (b) Cross view of the top of the cell, and (c) Cross view of the base of the cell (measurements in millimetres).

2.3. Electrochemical Methods

Single and Double Loop Reactivation Potentiokinetic tests were carried out in the minicell in order to observe the surface evolution of Alloy 900 during the electrochemical tests. The electrolyte employed for the reactivation tests was 2 M H_2SO_4, 0.01 M KSCN, and 0.5 M NaCl [24, 25]. In the single loop method, the specimen was passivated at 240 mV vs Ag/AgCl with 3 M KCl electrode for two minutes. Later, the potential decreased down to the open circuit potential at 1.667 mV/s. A measure of the degree of sensitisation could be obtained by calculating the reactivation charge [26]. In the double loop method, the Open Circuit Potential (OCP) was measured for two minutes. Next, the work electrode was anodically polarised from OCP to 340 mV vs Ag/AgCl with 3M KCl electrode at a rate of 1.667 mV/s; this is the activation loop. Then, the scanning direction was reversed and the potential decreased at the same rate until reaching OCP; this is the reactivation loop. The ratio between charges in the reactivation (Qr) and the activation (Qa) loop was used to measure the degree of sensitisation (DOS).

$$DOS(\%) = Qr / Qa \qquad (1)$$

The specimens could be classified into different levels of sensitisation (unsensitised, slightly sensitised, medium sensitised or severely sensitised) depending on their sensitisation degree and reactivation charge using different correlations, such as Cihal or the standard ASTM G-108 proposed in the literature [26, 27]. Images of the electrode surface during electrochemical tests were acquired in-situ using the confocal microscope in order to correlate these microscopic images with the electrochemical signal.

2.3. Microscopic analysis

In order to estimate the formation of new phases during the heat treatment, the materials were examined by scanning electron microscopy (SEM) and backscattered electrons. In addition, the samples were studied by X-ray diffraction (XRD) and energy dispersive X-ray analysis (EDX) in order to identify the new formed phases.

3. RESULTS AND DISCUSSION

3.1. Analysis by SEM, EDX, and XRD

Figure 3 shows micrographs of Alloy 900 in its as-received and sensitised (heated at 825 ºC for 1 hour) state obtained by SEM and backscattered electrons.

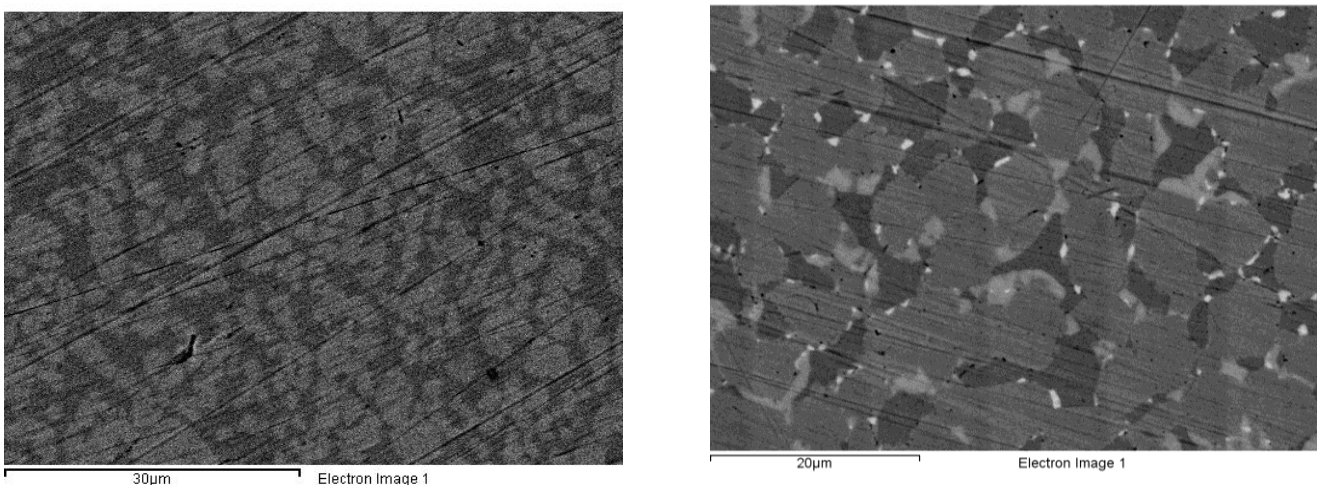

Figure 3. Back-Scattered electron images of Alloy 900 in its as-received and sensitised state (heated at 825 ºC during 1 hour).

Austenite, the light phase, and ferrite (α), the dark phase, are visible in Figure 3 a). Heat treatment causes the formation of two clear new phases (the brightest phases) and the drop in the

ferrite percentage value, as shown in Figure 3 b). According to the bibliography [24, 25, 28-30], the new phases can be identified like sigma and chi phases, the brightest being the chi phase. The phase percentage in every sample has been obtained by image analysis (using the "ImageJ" software), results are shown in Table 1; Alloy 900 in the as-received state only shows two phases, ferrite and austenite, the phase percentage being 46.10 % and 53.20 %, respectively. On the other hand, in the sensitised sample two new phases appear, the sigma and chi phases. In this case the percentages of phases are: 59.34 % of austenite phase, 20.21 % of ferrite phase, 19.01 % of sigma phase, and 1.44 % of chi phase. According to the literature [24, 31-34], the ferrite phase is the promoter of new phases and this is the reason why the percentage of this phase decreases.

The results of the EDX analysis (Table 1) show that the new phases present higher content of in Cr and Mo. This result is in agreement with the sigma phase composition reported in the literature [24, 25, 30, 32]. The chi phase has the highest content in molybdenum.

Table 1. Phase percentage and chemical compositions (wt %) in Chromium, Nickel, and Molybdenum of austenite (γ), ferrite (α), sigma (σ), and chi (χ) phases measured using EDX for the as-received and sensitised Alloy 900.

Phase	**As-received Alloy 900**			**Sensitised Alloy 900 (825 °C, 1 hour)**		
	Phase percentage (%)	Chemical composition (wt %)		Phase percentage (%)	Chemical composition (wt %)	
Austenite (γ)	53.20	% Cr	23.61	59.34	% Cr	23.71
		% Ni	5.46		% Ni	5.57
		% Mo	1.50		% Mo	1.61
Ferrite (α)	46.10	% Cr	26.03	20.21	% Cr	27.51
		% Ni	3.78		% Ni	2.56
		% Mo	2.30		% Mo	1.60
Sigma (σ)	0.00	% Cr	--	19.01	% Cr	30.92
		% Ni	--		% Ni	2.62
		% Mo	--		% Mo	3.43
Chi (χ)	0.00	% Cr	--	1.44	% Cr	27.74
		% Ni	--		% Ni	2.40
		% Mo	--		% Mo	8.22

In order to confirm the identity of the new formed phases an X-ray diffraction analysis has been carried out with Alloy 900 in its as-received and sensitised state. Figure 4 shows the spectra of X-ray diffraction. According to the literature [35-37], the peaks that appear between a ferrite peak and austenite peak in the interval from 40 to 50 grades (2θ) is related to the sigma phase. Therefore, one of the phases formed can be identified with the sigma phase.

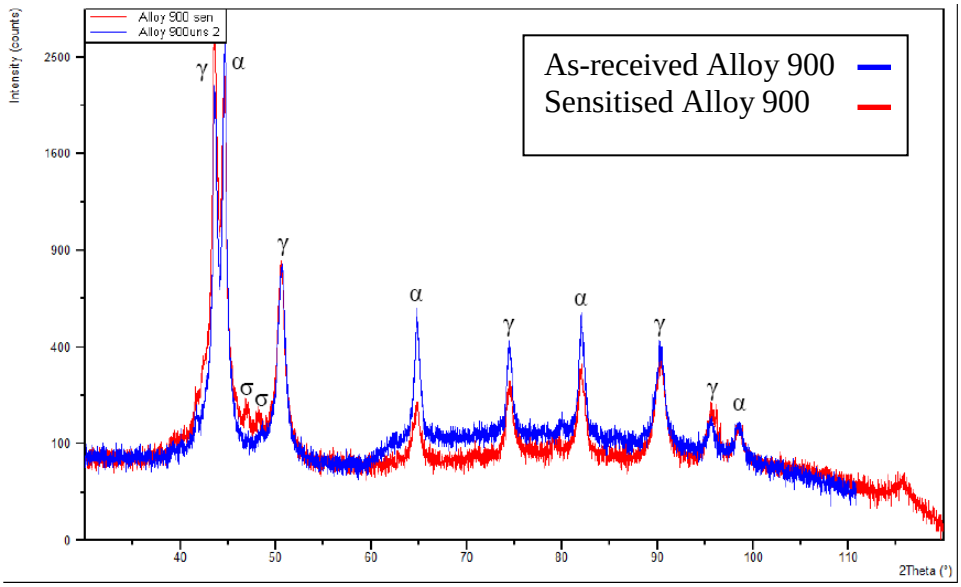

Figure 4. Spectrums of X-ray diffraction for Alloy 900 in its as-received and sensitised state (heated at 825 ºC during 1 hour).

3.2. Single loop reactivation potentiokinetic tests

Figure 5 shows single loop curves for Alloy 900 in its as-received and sensitised state (heated at 825 ºC during 1 hour). In-situ images of the electrode surface during the electrochemical tests have been obtained by confocal microscopy at the open circuit potential (OCP), during the potentiostatic step, and at different points of the reactivation curve, these points have been marked with letters in the curves of Figure 5. These images are presented in Figures 6 and 7.

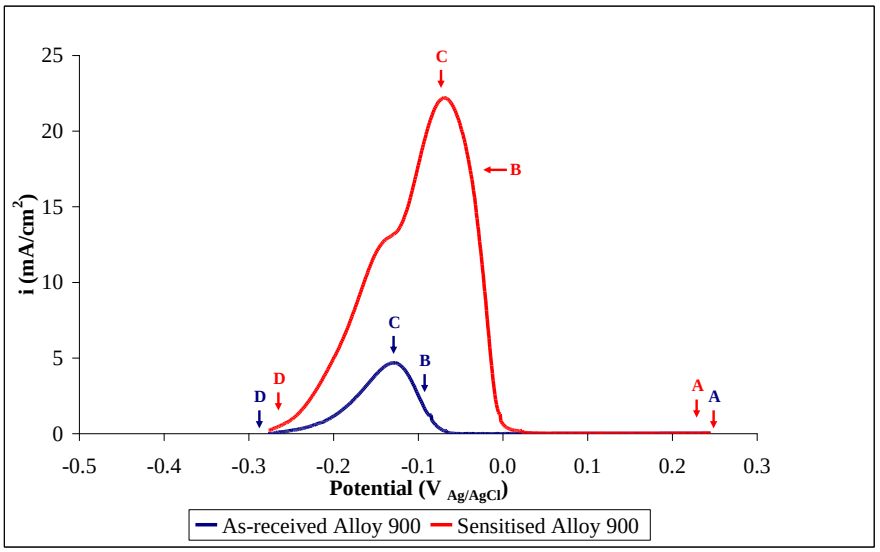

Figure 5. Single loop curves for Alloy 900 in the as-received and sensitised state (heated at 825 ºC for 1 hour).

In the reactivation curves of the single loop test, the reactivation charge is higher for the sensitised sample than for the as-received sample, as shown in Figure 5**.** Furthermore, in the sensitised sample two peaks appear during the reactivation curve.

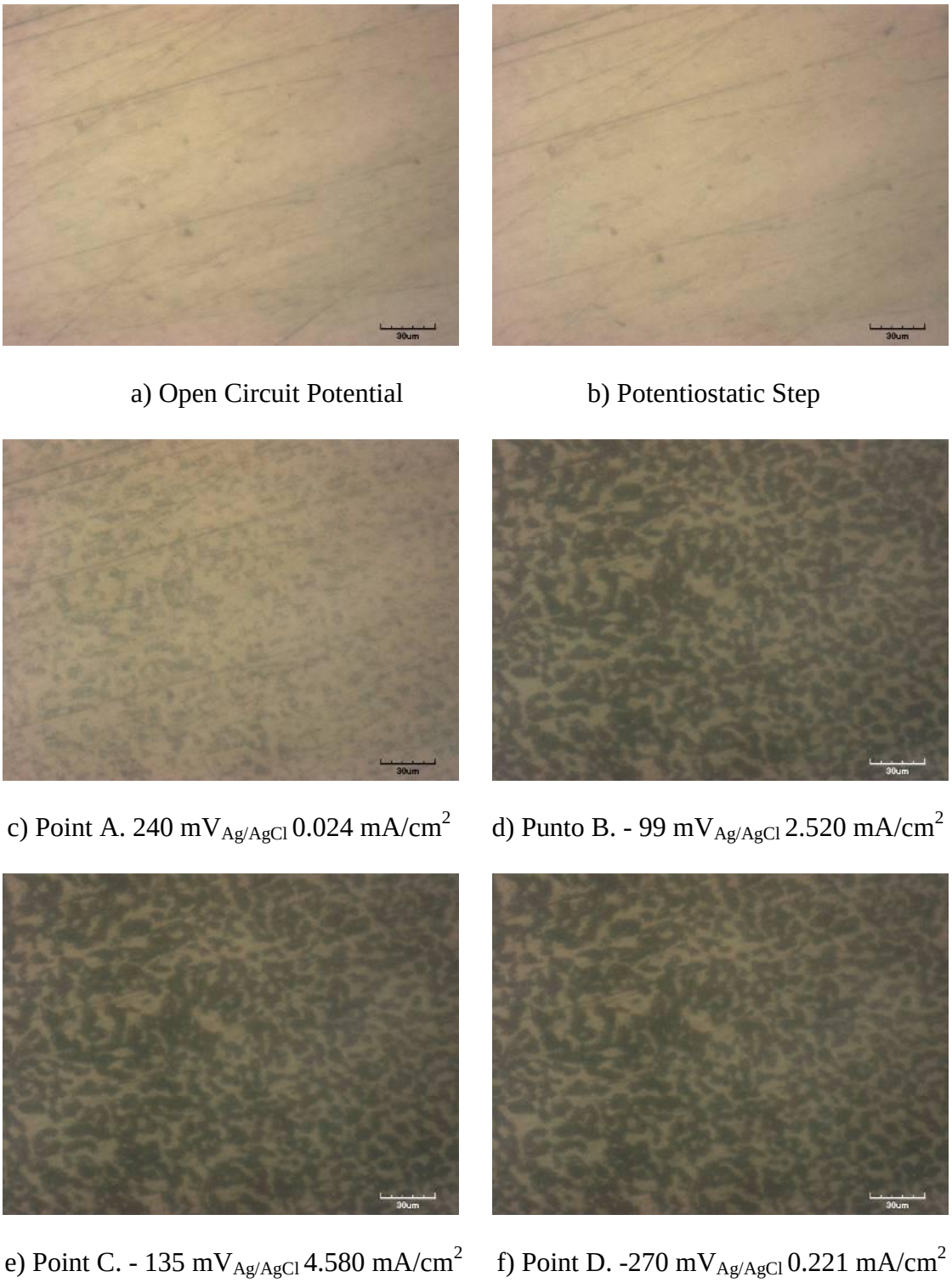

a) Open Circuit Potential b) Potentiostatic Step

c) Point A. 240 $mV_{Ag/AgCl}$ 0.024 mA/cm^2 d) Punto B. - 99 $mV_{Ag/AgCl}$ 2.520 mA/cm^2

e) Point C. - 135 $mV_{Ag/AgCl}$ 4.580 mA/cm^2 f) Point D. -270 $mV_{Ag/AgCl}$ 0.221 mA/cm^2

Figure 6. Images of the Alloy 900 in the as-received state during the single loop test obtained by means of the confocal microscope (500x).

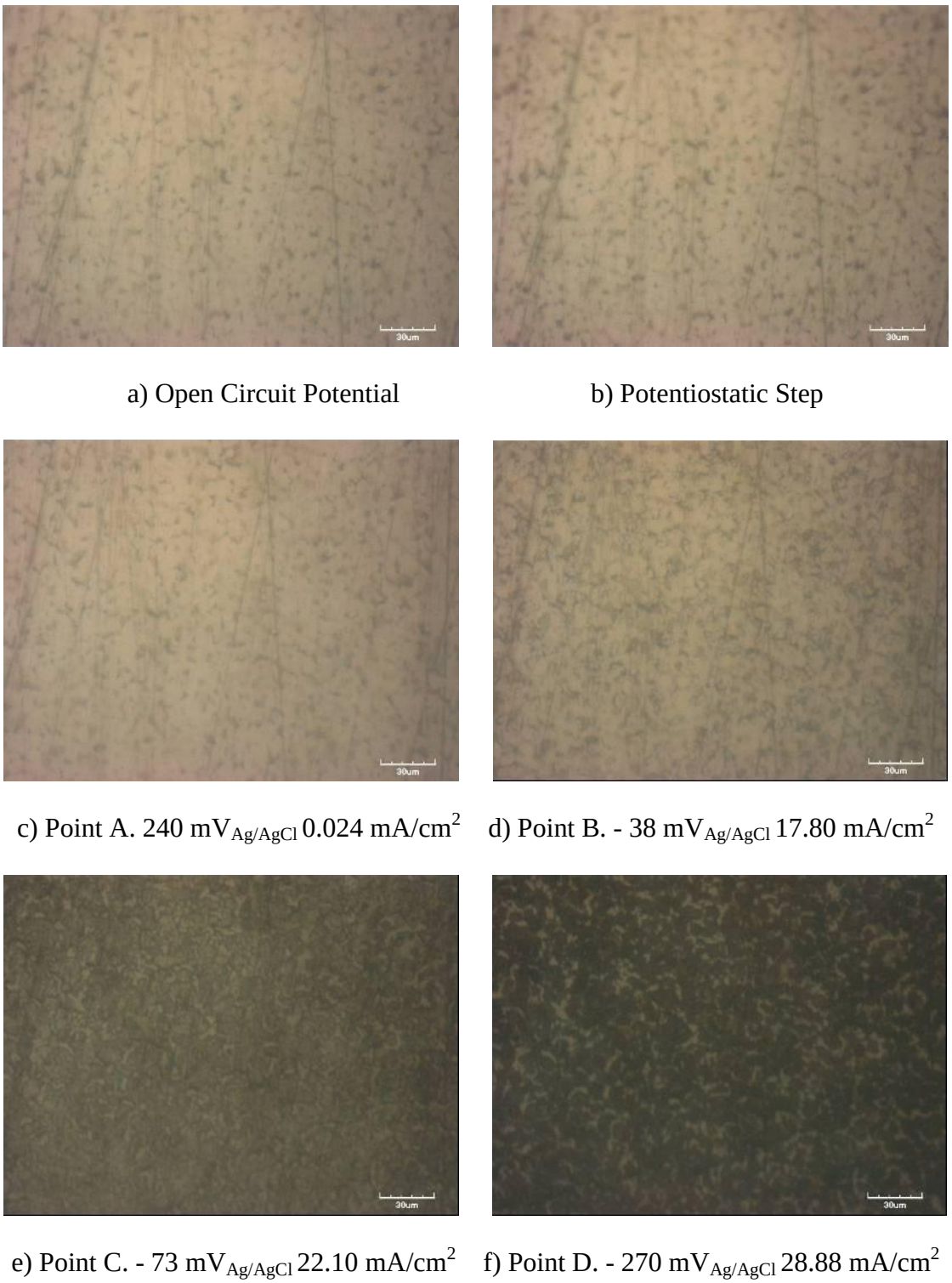

a) Open Circuit Potential b) Potentiostatic Step

c) Point A. 240 $mV_{Ag/AgCl}$ 0.024 mA/cm^2 d) Point B. - 38 $mV_{Ag/AgCl}$ 17.80 mA/cm^2

e) Point C. - 73 $mV_{Ag/AgCl}$ 22.10 mA/cm^2 f) Point D. - 270 $mV_{Ag/AgCl}$ 28.88 mA/cm^2

Figure 7. Images of the Alloy 900 in the sensitised state (heated at 825 ºC during 1 hour) during the single loop test obtained by means of the confocal microscope (500x).

The evolution of the electrode surface during the single loop tests is different between the as-received Alloy 900 and the sensitised Alloy 900, as shown in Figures 6 and 7. In the case of the sensitised sample, its immersion in the electrolyte during the open circuit potential measure produces the attack in some areas of the surface. However, the surface of the as-received sample remains

unaffected during the open circuit potential step. Later, during the potentiostatic step, the as-received specimen remains unaffected; on the other hand, in the sensitised sample the attack in the affected areas becomes more marked. Figure 8 shows the registry of the current density of Alloy 900 in its as-received and sensitised state during the potentiostatic test. Current density is higher in the sensitised specimen than in the unsensitised specimen due to the attacked areas observed in the sensitised sample.

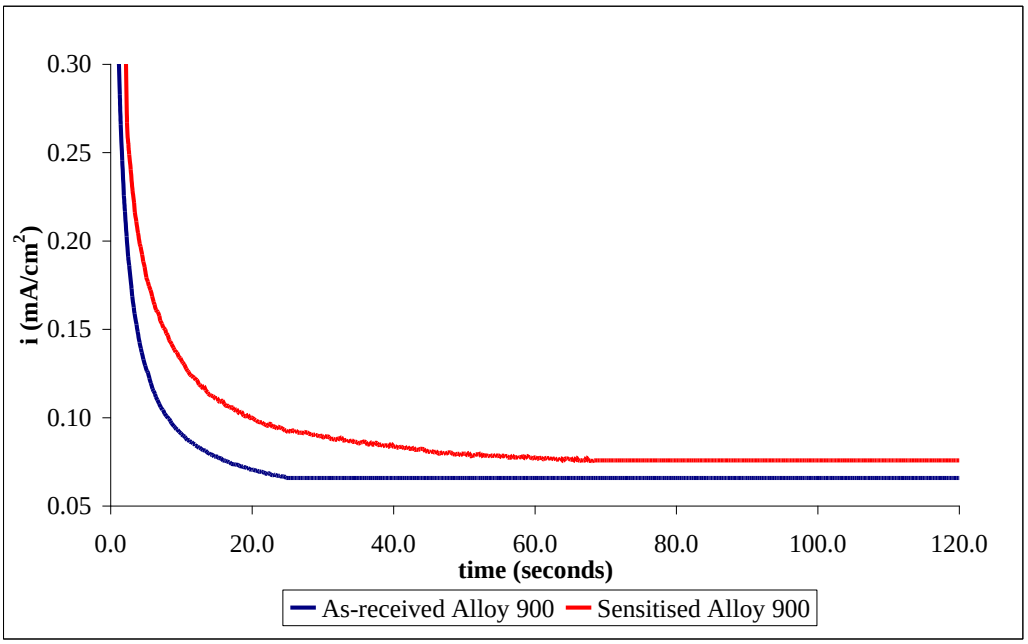

Figure 8. Registry of current density of Alloy 900 in the as-received and sensitised state (heated at 825 ºC during 1 hour) during the potentiostatic step.

After the potentiostatic tests, the reactivation curves were carried out. Figures 6 c) and 7 c) show the electrode surface at point A (beginning of the curve) of the reactivation curves. In the case of the as-received sample, the ferrite phase begins to be attacked and becomes darker, while the austenite phase remains unaffected. According to the literature, the ferrite phase is less corrosion resistant than the austenite phase in a large number of environments [23, 38-40]. The attack to the ferrite phase grows with the increase in the current density of the reactivation curve, while the austenite remains unaffected. When the point of maximum density of the reactivation curve is reached (point C), the ferrite phase is completely attacked (Figure 6 e)). After that, and until the end of the test, the surface remains without visible changes. In the sensitised sample, the attack grows in the previously revealed areas. Damage grows surrounding some areas that remain unaffected. When the point of maximum current density (point C) is reached, the entire surface is affected, except the areas that have been surrounded by the damage (Figure 7 e)). After this point no visible changes can be observed on the surface of the sensitised Alloy 900. On the other hand, the presence of one peak in the reactivation curve of the as-received sample can now be related to the attack to only one of the phases (ferrite phase). In the case of the sensitised Alloy 900, the presence of two peaks in the reactivation curve of

the sensitised sample could be related to the attack to the austenite and ferrite phases, because only a small area of the surface remains unaffected.

The percentage of the affected area for every sample during reactivation curves can be calculated by image analysis in order to relate the differences in the reactivation charge with the changes observed on the electrode surface. Furthermore, it is possible to evaluate the normalised charge, because the area affected during the tests is known. Table 2 summarises the values of the reactivation charge, the affected area, and the normalised reactivation charge obtained during the single loop tests for Alloy 900 in its as-received and sensitised states.

Table 2. Reactivation charge values, affected area during the single loop tests, normalised charge values for the Alloy 900 in its as-received and sensitised state (heated at 825 ºC for 1 hour).

Sample	Reactivation Charge (C/cm^2)	Affected Area (cm^2)	Normalised Reactivation Charge (C/cm^2)
As-received Alloy 900	0.148	9.89×10^{-3}	0.323
Sensitised Alloy 900	1.501	17.06×10^{-3}	1.900

According to the correlations of the ASTM G-108 [26], the sample heated at 825 ºC for 1 hour shows a sensitised structure and the as-received Alloy 900 shows a slightly sensitised structure. The percentage of area affected during the single loop test with the as-received Alloy 900 (45.70 %) is similar to the percentage of ferrite phase observed in the SEM images (46.10 %). On the other hand, the percentage of unaffected area observed during the single loop test carried out with the sensitised sample (21 %) is similar to the percentage of new phases formed during heating (20.45 %). Furthermore, the attack in the sensitised sample grows surrounding these areas. Therefore, the formation of new phases (sigma and chi) that are rich in alloying elements, such as Cr and Mo, lead to the depletion of these elements in the nearby areas. The corrosion resistance of the new phases is higher than the rest of the phases and the attack grows surrounding these new phases, which remain unaffected. This behaviour is in accordance with the literature, because the areas more sensitive to corrosion attack in a sensitised specimen are the depleted zones close to the new intermetallic precipitates [24, 25, 30, 32, 34, 41-44].

3.3. Double loop reactivation potentiokinetic tests

Figure 9 shows the double loop curves for Alloy 900 in its as-received and sensitised state (heated at 825 ºC during 1 hour). In the same way as in the single loop tests, in-situ images of the electrode surface during the electrochemical tests have been obtained by confocal microscopy at the open circuit potential (OCP) and at different points of the reactivation curves, these points have been marked with letters in the curves of Figure 9. The images are presented in Figures 10 and 11.

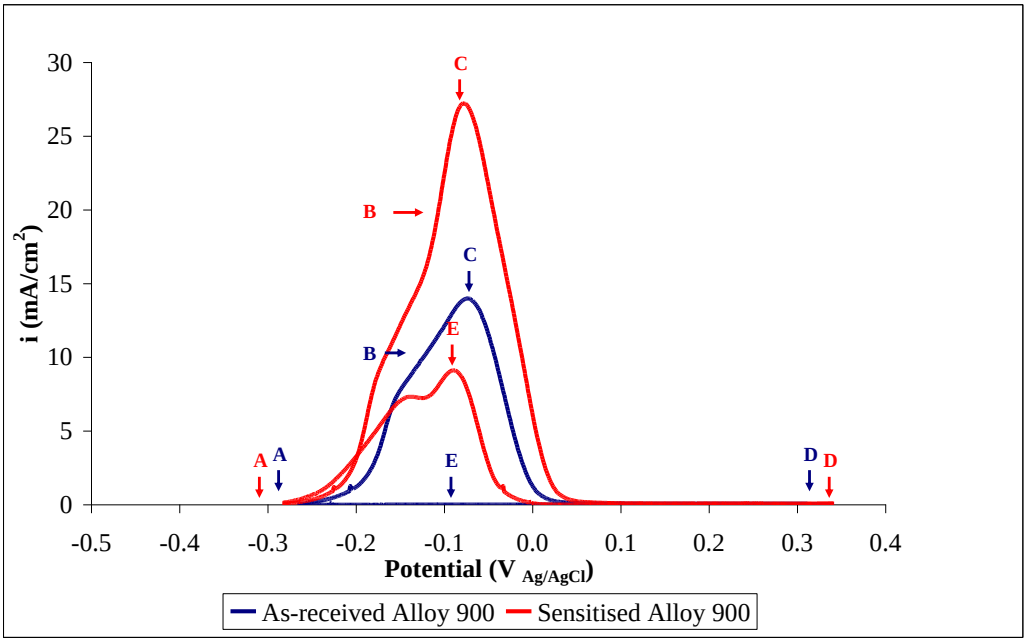

Figure 9. Double loop curves for Alloy 900 in the as-received and sensitised state (heated at 825 ºC for 1 hour).

The activation and reactivation charges obtained during the double loop tests are higher for the sensitised sample than for the unsensitised sample. The degree of sensitisation calculated according to equation 1 for the as-received and sensitised sample is 0.00 % and 33.78 %, respectively. According to Cihal [27], the degree of sensitisation of the sensitised sample corresponds to a highly sensitised specimen. On the other hand, during the reactivation charge of the sensitised specimen two peaks are observed, while in the case of the as-received sample, only one peak appears.

Figures 10 and 11 show clear differences in the evolution of the surface between the as-received and sensitised Alloy 900. The exposure of the sensitised sample to the electrolyte produces etching in the same areas as those revealed in the single loop test (Figure 11 a)).

On the other hand, the as-received sample does not show visible changes after the open circuit potential measure (Figure 10 a)). During the activation branch, when the current density increases, the ferrite phase begins to be revealed in the as-received sample (Figure 10 b)). In the case of the sensitised Alloy 900, the attack to previously marked areas grows and the entire surface begins to be dark, except for some zones that were surrounded by the initially attacked areas and now remain unaffected (Figure 11 b)).

These areas could correspond to the new areas formed during the heat treatment. In the as-received sample, when the maximum current density during the activation branch is reached, ferrite phase is completely attacked and the limits between austenite and ferrite are clearly visible (Figure 10 c)). On the other hand, when the maximum current density of the activation branch of the sensitised sample is reached, in the electrode surface only the new phases remain unaffected, while the rest of the surface becomes darkened and the adjacent areas to the new phases are the most severely attacked (Figure 11 c)).

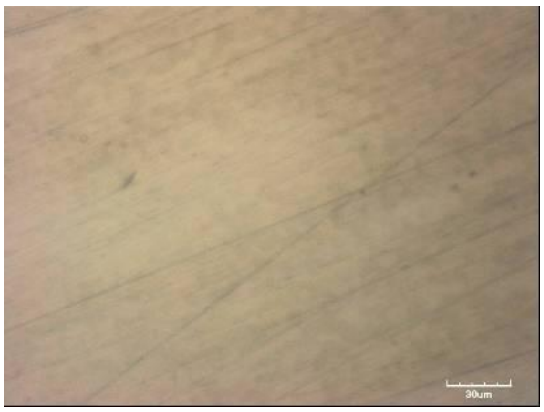

a) Point A. -283 $mV_{Ag/AgCl}$ 0.022 mA/cm^2

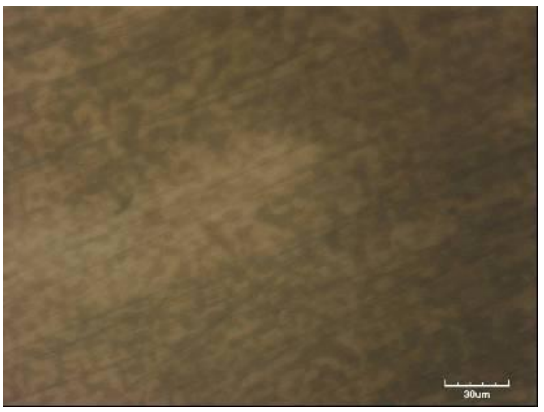

b) Point B. -120 $mV_{Ag/AgCl}$ 10.31 mA/cm^2

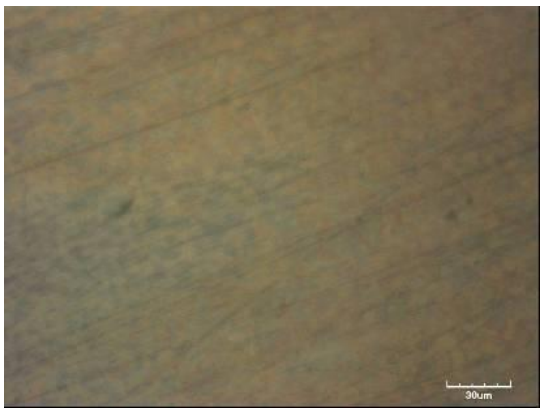

c) Point C. -68 $mV_{Ag/AgCl}$ 13.90 mA/cm^2

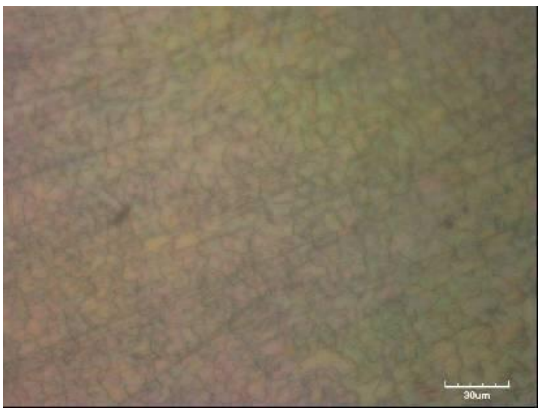

d) Point D. 333 $mV_{Ag/AgCl}$ 0.025 mA/cm^2

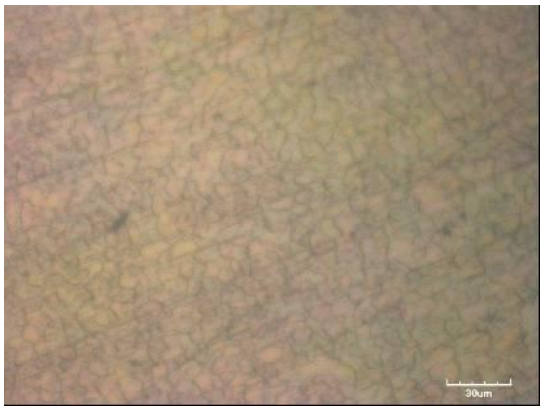

e) Point E. - 94 $mV_{Ag/AgCl}$ 0.074 mA/cm^2

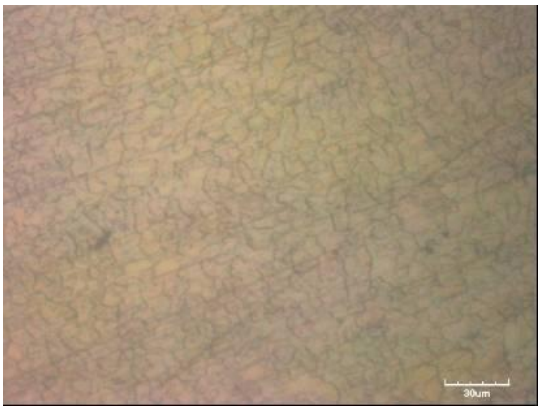

f) End of the test. - 283 $mV_{Ag/AgCl}$ 0.017 mA/cm^2

Figure 10. Images of the Alloy 900 in the as-received state during the double loop test obtained by means of the confocal microscope (500x).

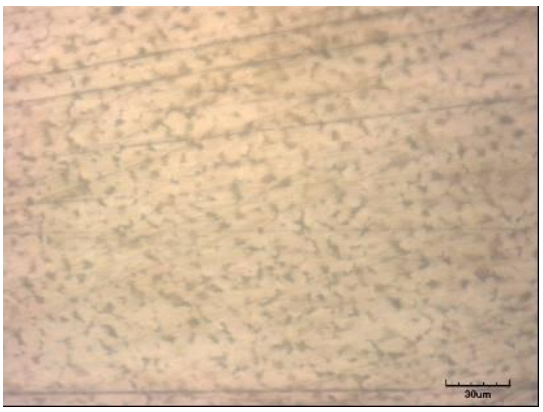

a) Point A. -283 $mV_{Ag/AgCl}$ 0.020 mA/cm^2

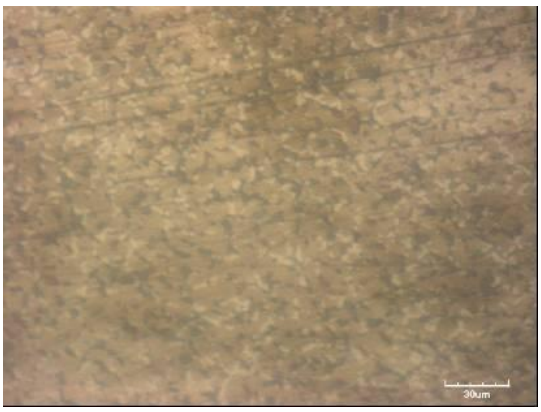

b) Point B. -108 $mV_{Ag/AgCl}$ 19.51 mA/cm^2

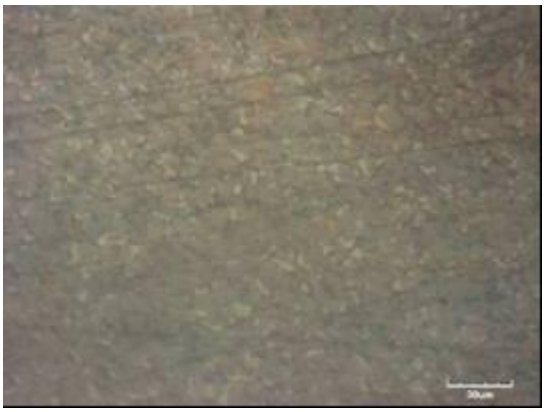

c) Point C. - 72 $mV_{Ag/AgCl}$ 27.90 mA/cm^2

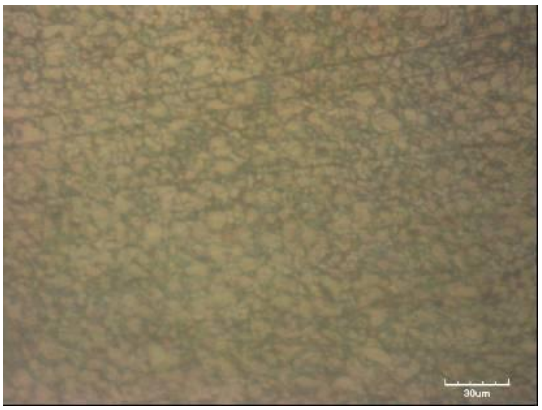

d) Point D. 333 $mV_{Ag/AgCl}$ 0.075 mA/cm^2

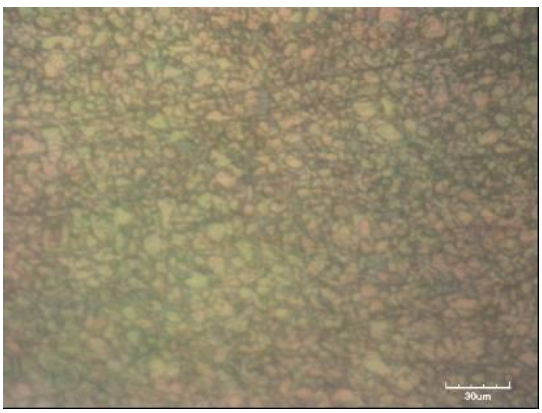

e) Point E. - 96 $mV_{Ag/AgCl}$ 8.87 mA/cm^2

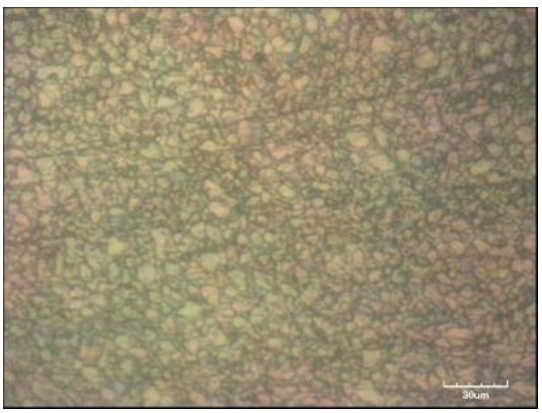

f) End of the test. - 283 $mV_{Ag/AgCl}$ 0.020 mA/cm^2

Figure 11. Images of the Alloy 900 in the sensitised state during the double loop test obtained by means of the confocal microscope (500x).

When the current density of the activation branch begins to decrease, a patina of colour appears on the electrode surface in both samples (the as-received and the sensitised Alloy 900), Figures 10 d)

and 11 d). The formation of this patina could be related to a passivation process and it could explain the decrease in current density. The main difference in the images obtained during the reactivation branch between the as-received and the sensitised sample is the formation of dark areas between grains in the case of the sensitised sample. These areas are the same zones as those attacked at the beginning of the test. Furthermore, these dark areas become more marked during the reactivation branch, as shown in Figures 11 e) and f). Then, these affected areas during the reactivation branch could be zones with a poor passive film, which leads to an increase in the reactivation charge. On the other hand, in the case of the as-received sample no visible variations are observed during the reactivation branch, Figures 10 e) and f), and the reactivation charge remains with a low value. Therefore, the differences observed in the electrochemical data can be related to the differences in the evolution of the electrode surface during the tests. The sensitised Alloy 900 presents new phases formed during heating that cause the depletion of alloying elements in the adjacent areas, and a higher attack during the activation branch accompanied by a higher activation charge than in the as-received sample. Furthermore, during the reactivation branch these depleted areas are attacked again leading to an increase in the reactivation charge.

4. CONCLUSIONS

The conclusions of this research may be summarised as follows:

1. The single and double loop reactivation methods are different. In the case of the single loop reactivation test, phases are revealed after the passivation process, except in the case of the sensitised sample, where a percentage of the surface is revealed in contact with the electrolyte. However, in the double loop reactivation tests, phases are revealed during the activation branch before the passivation process. Furthermore, the passive film is different in the single loop method than in the double loop method.
2. In the as-received Alloy 900, the ferrite phase is revealed during the reactivation branch in the single loop method and during the activation branch in the double loop method. The austenite phase remains unaffected.
3. In the sensitised specimen, the sensitisation process is due to the formation of new phases (sigma and chi) that deplete the alloying elements (Cr and Mo) in the adjacent areas. When the specimen is in contact with the electrolyte the zones adjacent to the new intermetallic phases are revealed.
4. In the sensitised specimen the attack during the reactivation tests grows around the new intermetallic phases that remain unaffected. In the single loop test the attack happens during the reactivation branch. In the double loop test, the attack happens during the activation branch and later during the reactivation branch in the depleted areas.
5. The affected area during the reactivation test is higher in the sensitised sample than in the as-received sample. In the as-received sample only one peak is observed during the reactivation curve because only one of the phases is attacked. On the other hand, in the sensitised sample,

two peaks are observed during the reactivation curve because the austentite and the ferrite phases are attacked and only the newly formed phases remain unaffected.

6. The use of the minicell can be useful in the characterisation of the sensitisation degree because it can provide additional information about the sensitisation behaviour during the electrochemical tests.

ACKNOWLEDGEMENTS

We wish to express our gratitude to MICINN (CTQ2009-07518), to FEDER, to the Generalitat Valenciana for its help in the CLSM acquisition (MY08/ISIRM/S/100), and to Dr. Asunción Jaime for her translation assistance.

References

1. A.S. Lima, A.M. Nascimento, H.F.G. Abreu, P. De Lima-Neto. *J. Mat. Sci.* 40 (2005) 139-144.
2. A.S.M. Paroni, N. Alonso-Falleiros, R. Magnabosco. *Corrosion* 62 (2006) 1039-1046.
3. Ching-An Huang, Yau-Zen Chang, S.C. Chen. *Corros. Sci.* 46 (2004) 1501-1513.
4. W.J. Lee, S.I. Pyun, J.W. Yeon, K.S. Chun, I.K. Choi. *Electrochemical Methods in Corrosion Research VI*, 289-2 (1998) 915-924.
5. M. Matula, L. Hyspecka, M. Svoboda, V. Vodarek, C. Dagbert, J. Galland, Z. Stonawska, Ludec Tuma. *Mat. Charact.* 46 (2001) 203-210.
6. N. Parvathavarthini, R.K. Dayal, H.S. Khatak, V. Shankar, V. Shanmugan. *J. Nucl. Mat.* 355 (2006) 68-82.
7. H. Shaikh, G. George, F. Shneider, K. Mummert, H.S. Khatak. *Transactions of the Indian Institute of Metals* 54 (2001) 27-39.
8. R. Leiva-Garcia, M.J. Muñoz-Portero, J. García-Antón. *Corros. Sci*. 52 (2010) 950-959.
9. T. Poormina, Jagannath Nayak, A. Nityananda Shetty. *Int. J. of Electrochem. Sci.* 5 (2010) 56-71.
10. Shun-Xin Li, Lei-Li, Shu-Rong Yu, R.Akid, Hong-Bo Xia. *Corros.Sci.* 53 (2011) 99-104.
11. R. Leiva-Garcia, M.J. Muñoz-Portero, J. García-Antón. *Int. J. of Electrochem. Sci.* 6 (2011) 442-460.
12. ASTM international. ASTM A -262. (2004).
13. I.Chattoraj, A.K. Bhattamishra, S. Jana, S.K. Das, S.P. Chakraborty, P.K. De. *Corros. Sci.* 38 (1996) 957-969.
14. S. Frangini, A. Mingnone. *Corrosion* 48 (1992) 715-726.
15. H. Sidhom, T. Amadou, H. Sahlaoui, C. Braham. *Metall. Mater Trans*. 38A (2007) 1269-1280.
16. H. Kanematsu, T. Kobayashi, K. Murakami, T. *Corrosion Reviews* 18, (2000) 53-64.
17. R. Leiva-Garcia, J. García-Antón, M.J. Muñoz-Portero. *Corros. Sci*. 51**,** (2009) 2080-2091.
18. Mojtaba Momeni. Corros. Sci. 52 (2010) 2653-2660.
19. J. García Antón, A. Igual Muñoz, J.L. Guiñón, V. Pérez Herranz. Electro-Optical Method by On-line Visualization of Electrochemical Process and Experimental Process. Spain P-200002525 (2000).
20. J. García Antón, A. Igual Muñoz, J.L. Guiñón, V. Pérez Herranz. Horizontal Electrochemical Cell by the Electro-Optical Analysis of Electrochemical Process. Spain P-200002526(2000).
21. J. García Antón, A. Igual Muñoz, J.L. Guiñón, V. Pérez Herranz, J. Pertusa-Grau. *Corrosion* 59 (2003) 172-180.
22. J. García Antón, A. Igual Muñoz, J.L. Guiñón, V. Pérez Herranz. *J. Appl. Electrochem.* 31 (2001) 1195-1202.
23. R. Leiva-Garcia, J. García-Antón, M.J. Muñoz-Portero *Corros. Sci*. 52 (2010) 2133-2142.

24. C.J. Park, V. Shankar Rao, H.S. Kwon. *Corrosion* 61 (2005), 76-83.
25. K.N. Adhe, V. Kain, K. Madangopal, and H.S. Gadiyar. *J. Mat. Eng. Perform*. 5 (2007) 500-506.
26. ASTM international. ASTM G-108 (2004).
27. V. Cihal V. Materials Science Monographs 18. Intergranular corrosion of steels and alloys. Elsevier (1984).
28. Nathalie Lopez, Mariano Cid, Monique Puiggali, Iñaki Azkarate, Alberto Pelayo. *Mater. Sci. Eng. A-Struct. Mat. Prop. Microstruct Process A* 229 (1997) 123-128.
29. Joanna Michalska, Maria Sozanska. *Mater. Charact.* 56 (2006) 355-362.
30. Darlene Yuko Kobayashi, Stephan Wolynec. *Matherials research* 2 (1999).
31. Henrik Sieurin, Rolf Sandström. *Mater. Sci. Eng. A-Struct. Mat. Prop. Microstruct Process* A 444 (2007) 271-276.
32. Hozni M.Ezuber, A.El Houd, F. El-Shawesh. *Desalination* 207 (2007) 268-275.
33. K.M. Lee, H.S. Cho, D.C. Choi. *J. Alloy Compd*. 285, (1999) 156-161.
34. Yutaka S. Sato, Hiroyuki Kokawa.. *Scripta Mater*. 40 (1999) 659-663.
35. A.A.Guimarães, P. R. Mei. *Journal of Materials Processing Technology* 155–156 (2004) 1681-1689.
36. C.M. Souza Jr , H.F.G. Abreu, S.S.M. Tavares, J.M.A. Rebello. *Mater. Charact.* 59 (2008) 1301-1306.
37. Rodrigo Magnabosco. *Materials Research* 12 (2009) 321-327.
38. M. Femenia, J. Pan, C. Leygraf, P. Luukkonen. *Corros. Sci.* 43, (2001) 1939-1951.
39. Wen-Ta Tsai, Jhen-Rong Chen. *Corros. Sci.* 49 (2007) 3659-3668.
40. L.F. Garfias-Mesias, J.M. Sykes. *Corros. Sci.* 41 (1999) 959-987.
41. J.S. Kim, H.S. Kwon. *Corrosion* 55 (1999) 512-521.
42. A.Elhoud, H. Ezuber, W. Deans. *Materials and Corrosion* 61 (2010) 199-204.
43. Hyungsun Kim, JianFeng Yang, Tohru Sekino, Masakazu Anpo, Soo Wohn Lee. *Materials Science Forum* 658 (2010) 380-383.
44. N. Lopez, M. Cid, M. Puiggalli. Corros. Sci. 41 (1999) 1615-1631